iScience

CellPress
OPEN ACCESS

Article

Neurosensory anatomy and function in *Dimetrodon*, the first terrestrial apex predator

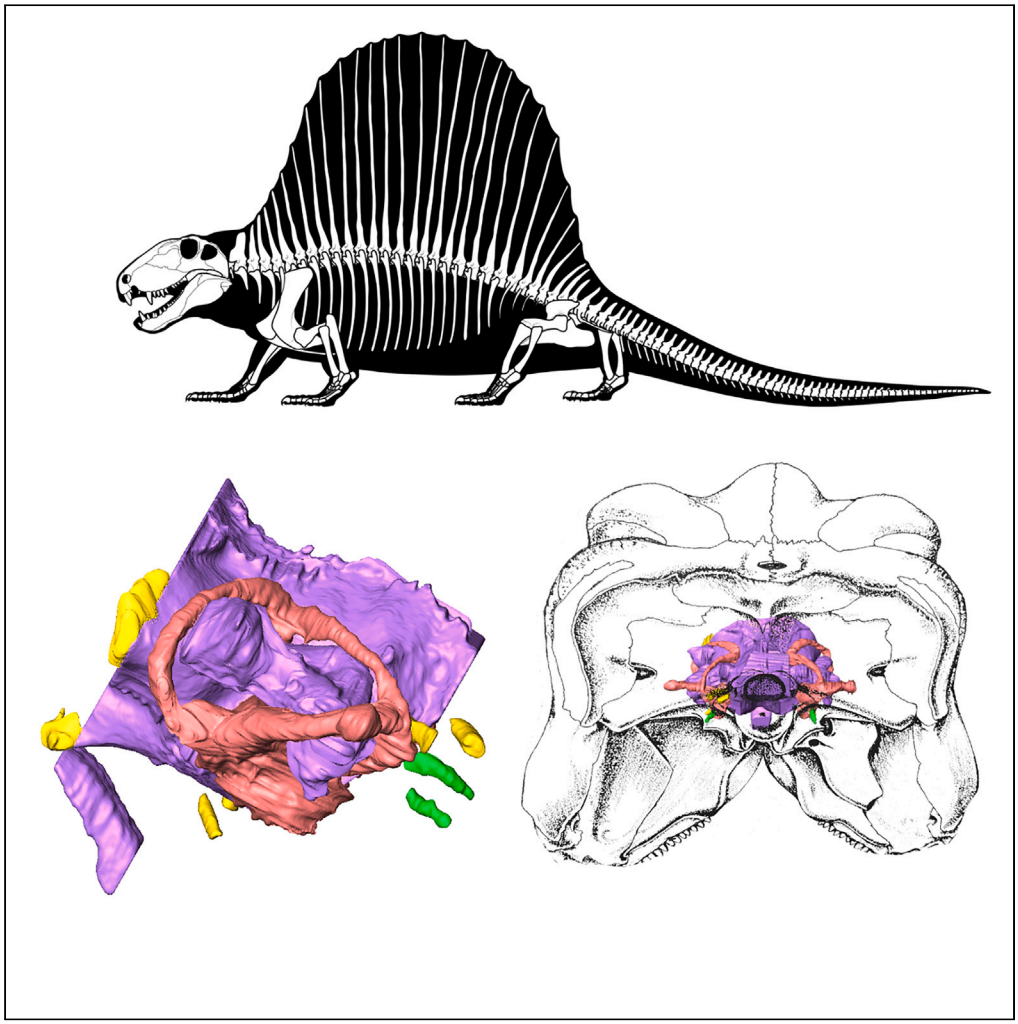

Kayla D. Bazzana-Adams, David C. Evans, Robert R. Reisz

kayla.bazzana@mail.utoronto.ca

Highlights

The brain of *Dimetrodon* is strongly flexed with highly enlarged floccular fossae

The inner ear of *Dimetrodon* is very well ossified with large ampullae

ASR results confirm *Dimetrodon* as representing the ancestral therapsid condition

Bazzana-Adams et al., iScience *26*, 106473
April 21, 2023 © 2023 The Authors.
https://doi.org/10.1016/j.isci.2023.106473

iScience

CellPress
OPEN ACCESS

Article

Neurosensory anatomy and function in *Dimetrodon*, the first terrestrial apex predator

Kayla D. Bazzana-Adams,[1,2,3,5,*] David C. Evans,[2,3] and Robert R. Reisz[1,4]

SUMMARY

***Dimetrodon* is among the most recognizable fossil taxa, as well as the earliest terrestrial amniote apex predator. The neuroanatomy and auditory abilities of *Dimetrodon* has long been the subject of interest, but palaeoneurological analyses have been limited by the lack of three-dimensional endocast data. The first virtual endocasts reveal a strongly flexed brain with enlarged floccular fossae and a surprisingly well-ossified bony labyrinth clearly preserving the semicircular canals, along with an undifferentiated vestibule and putative perilymphatic duct. This first detailed palaeoneurological reconstruction reveals potential adaptations for a predatory lifestyle and suggests *Dimetrodon* was able to hear a wider range of frequencies than anticipated, potentially being sensitive to frequencies equal to or higher than many extant sauropsids, despite lacking an impedance matching ear. Ancestral state reconstructions support the long-standing view of *Dimetrodon* as representative of the ancestral state for therapsids, while underscoring the importance of validating reconstructive analyses with fossil data.**

INTRODUCTION

Crown mammals have highly derived brain and ear morphologies that readily distinguish them from other tetrapods.[1,2] The evolution of the mammalian brain and ear have been studied extensively,[2–5] and that interest has extended beyond crown mammals to non-mammalian therapsids, the clade that includes the closest extinct relatives of mammals.[6–10] However, the neuroanatomy of the pelycosaur-grade synapsids, the earliest members of the synapsid lineage, has received little attention; to date, the varanopids are the only non-therapsid synapsids whose neuroanatomy has been studied in comparable detail.[11,12]

The pelycosaur-grade synapsid *Dimetrodon* is one of the most iconic and best-known of all fossil taxa. Known primarily from the early Permian of North America,[13,14] *Dimetrodon* has an extended fossil record and is one of the earliest terrestrial apex predators.[14,15] As a sphenacodontid, *Dimetrodon* occupies an important position in synapsid phylogeny, being one of the closest relatives to Therapsida, yet still only approximately 20 million years from the beginning of the 316 million years long evolutionary history of the synapsids. Anatomical and paleobiological studies of *Dimetrodon* have included muscle reconstructions,[16] dental anatomy,[15] and osteohistology,[17] but studies of its palaeoneurology have been limited, despite its importance for understanding its sensory abilities and paleoecology.

The auditory abilities of *Dimetrodon*, and of pelycosaur-grade synapsids in general, have long been debated,[1,3,18,19] with the presence or absence of a postquadrate tympanum, and the impedance matching abilities implied therein, the subject of particular interest. The predominant view is that pelycosaur-grade synapsids lacked any form of distinct tympanic membrane, such that the mammalian tympanum and therefore, the impedance matching middle ear is not homologous to those of crown sauropsids[19]; however, little is known about the range of sounds that these earliest synapsids were able to hear. It has been suggested that if *Dimetrodon* could hear any form of airborne sound, it was only at very low frequencies, likely below 1000 Hz.[1,19] Researchers are now able test these functional hypotheses,[7,11] but this requires a thorough understanding of the palaeoneuroanatomy of the taxon in question, which in turn requires reconstruction of the relevant soft-tissue structures.

Previous neuroanatomical studies of *Dimetrodon* have been based primarily on the examination of osteological correlates,[14,20] focusing chiefly on the overall shape of the brain, and the positioning of cranial nerve foramina. Cursory descriptions of the inner ear have been given[1,14,20] but these descriptions have

[1]Department of Biology, University of Toronto Mississauga, Mississauga, ON, Canada

[2]Department of Natural History, Royal Ontario Museum, Toronto, ON, Canada

[3]Department of Ecology and Evolutionary Biology, University of Toronto, Toronto, ON, Canada

[4]International Center of Future Science, Dinosaur Evolution Research Center, Jilin University, Changchun, Jilin Province, China

[5]Lead contact

*Correspondence: kayla.bazzana@mail.utoronto.ca

https://doi.org/10.1016/j.isci.2023.106473

This is an open access article under the CC BY license (http://creativecommons.org/licenses/by/4.0/).

by necessity lacked detail. A physical cranial endocast of *Dimetrodon limbatus* has been described previously,[20–22] but this endocast does not preserve the semicircular canals or the paths of any cranial innervations. Further, the vestibular portion of the endocast, which is the only portion of the inner ear preserved in that specimen, includes the canal that connects the fenestra vestibuli to the vestibule, obscuring much of the vestibular morphology.[22] A wax endocast model of the inner ear of *Dimetrodon* that does include the labyrinth has been described previously,[23] but this model has never been figured in detail and is a reconstruction from a serially sectioned skull that has been scaled up in size from the original size of the labyrinth,[24] rendering it of limited utility for analyses that depend upon accurate measurements.

Here, we use micro-computed tomography to generate the first virtual endocast-based description of the brain and inner ear of any sphenacodontid and reveal more nuanced details of the neuroanatomy of *Dimetrodon* than were previously known. This new data allow estimation of the potential range of frequencies that *Dimetrodon* was able to hear, which has implications for the neurosensory function of this important early apex predator. We then conduct an ancestral state reconstruction to evaluate the evolution of four key neuroanatomical traits across synapsids.

Methods

Specimen

FMNH UC 423, isolated braincase referred to *Dimetrodon loomisi* Romer, 1937 by Romer and Price.[14] Specimen preserves supraoccipital-opisthotic complex, both prootics, parasphenoid plate, basioccipital, and left exoccipital.

Occurrence

Craddock Bonebed, Baylor County, Texas, U.S.A. Arroyo Formation, Clear Fork Group, 272–279 Ma (late Cisuralian).

Taxonomic assignment

FMNH UC 423 was assigned to *D. loomisi* by Romer and Price[14] based on the predominance of *D. loomisi* at the locality in which it was found; however, *D. limbatus* and *Dimetrodon natalis* are also known from the same locality.[14] The specific diagnosis for *D. loomisi* does not include braincase characters, so the species assignment of FMNH UC 423 should be considered tentative. However, generic assignment to *Dimetrodon* is confident based on (i) the predominance of *Dimetrodon* among Craddock sphenacodontid material, and (ii) the morphology of the paroccipital processes that differ substantially across the major clades of pelycosaur-grade synapsids. The processes in *Dimetrodon* are long, slim, and posterolaterally directed, in contrast to *Edaphosaurus* (long, broad, horizontally directed), *Ophiacodon* (short, horizontally directed), or *Casea* (short, very broad, horizontally directed).[14] Although the distal portions of both processes are missing in FMNH UC 423, the preserved proximal portions clearly indicate slim, posterolaterally directed structures, matching the condition described for *Dimetrodon* (Figure 1). Although *Secodontosaurus* is also known from the same locality, substantial differences in proportion easily distinguish between the two genera.[25]

Scanning

FMNH UC 423 was micro-CT scanned at the University of Chicago's PaleoCT facility at 150 kV and 400 μA, using a 1.0 mm Cu filter and a 0.5 mm Sn filter. A total of 1500 projections were taken over a total scan time of 1 h 40 min, producing a final voxel size of 60.07 × 60.07 × 60.07 μm.

Three-dimensional renderings of the cranial and otic endocasts were produced by manual segmentation in AVIZO Lite 9.7.0. Bony labyrinth measurements were taken following the protocol of Benoit et al.[7] Ellipticity was calculated using the equation given by Goyens.[26] Hearing range estimates were calculated using the equations of Walsh et al.[27] Unprocessed 16-bit TIFF slices are available online through MorphoSource (https://www.morphosource.org/concern/media/000441468?locale=en).

Ancestral state reconstruction

Ancestral state reconstruction (ASR) analyses were conducted under both (i) a maximum likelihood (ML) framework in *R* (v.4.1.3) using the *ace* function from the package *ape*,[28] which employs an equal rates model

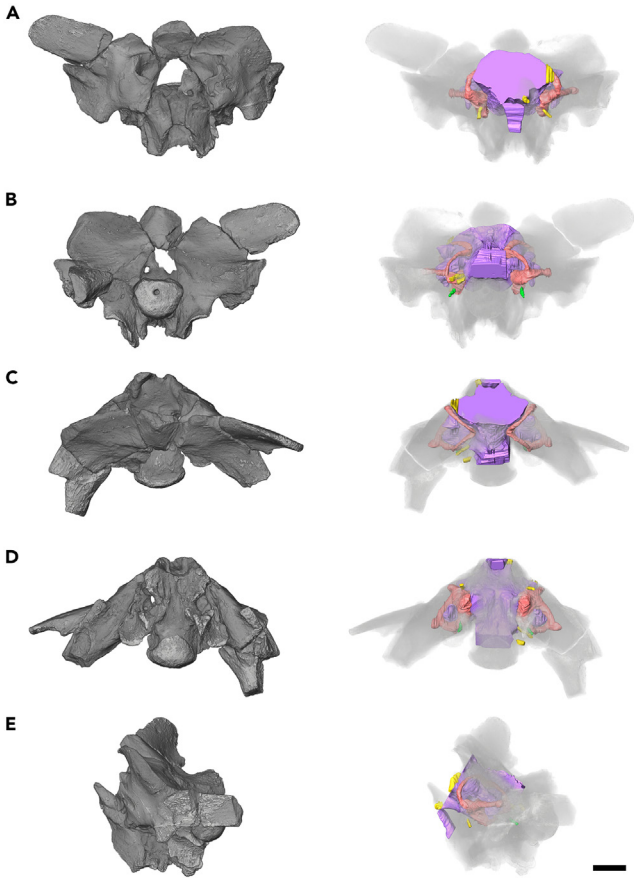

Figure 1. Braincase of *Dimetrodon*

Opaque and semi-transparent volume renderings of FMNH UC 423 with endocast in (A) anterior, (B) posterior, (C) dorsal, (D) ventral, and (E) left lateral views. Scale bar equals 1 cm.

to estimate marginal ancestral states, and (ii) a maximum parsimony (MP) framework in *Mesquite*. Reconstructions were performed on a time-scaled phylogenetic tree of fossil synapsids,[29] with a final sample of 32 taxa representing the majority of the major synapsid clades. All taxa were coded for the degree of brain flexure, flocculus size, presence and morphology of the secondary common crus, and the presence of a distinct cochlear recess.

Brain flexure was measured as the angle at the hypophyseal fossa, following the protocol of Macrini et al.[30] Flocculus size was coded as (0) small/discrete bump that only just extends into the space defined by the anterior semicircular canal, or (1) large/pronounced protrusion extending past the anterior canal. Secondary common crus morphology was coded as (0) absent, (1) short and broad, or (2) elongate and narrow. The cochlear recess was coded as (0) absent or (1) present. The complete dataset used for the analyses is available in the supplemental information.

Institutional abbreviations

FMNH UC, Field Museum of Natural History, Chicago, U.S.A.

Anatomical abbreviations

aasc, ampulla of the anterior semicircular canal; alsc, ampulla of the lateral semicircular canal; asc, anterior semicircular canal; cc, common crus; CN.V, trigeminal nerve; CN.VI, abducens nerve; CN.VII, facial nerve; CN.IX-XI, metotic foramen; CN.XII, hypoglossal nerve; ff, floccular fossa; lsc, lateral semicircular canal; pd, perilymphatic duct; pf, pituitary fossa; psc, posterior semicircular canal; scc, secondary common crus; v, vestibule.

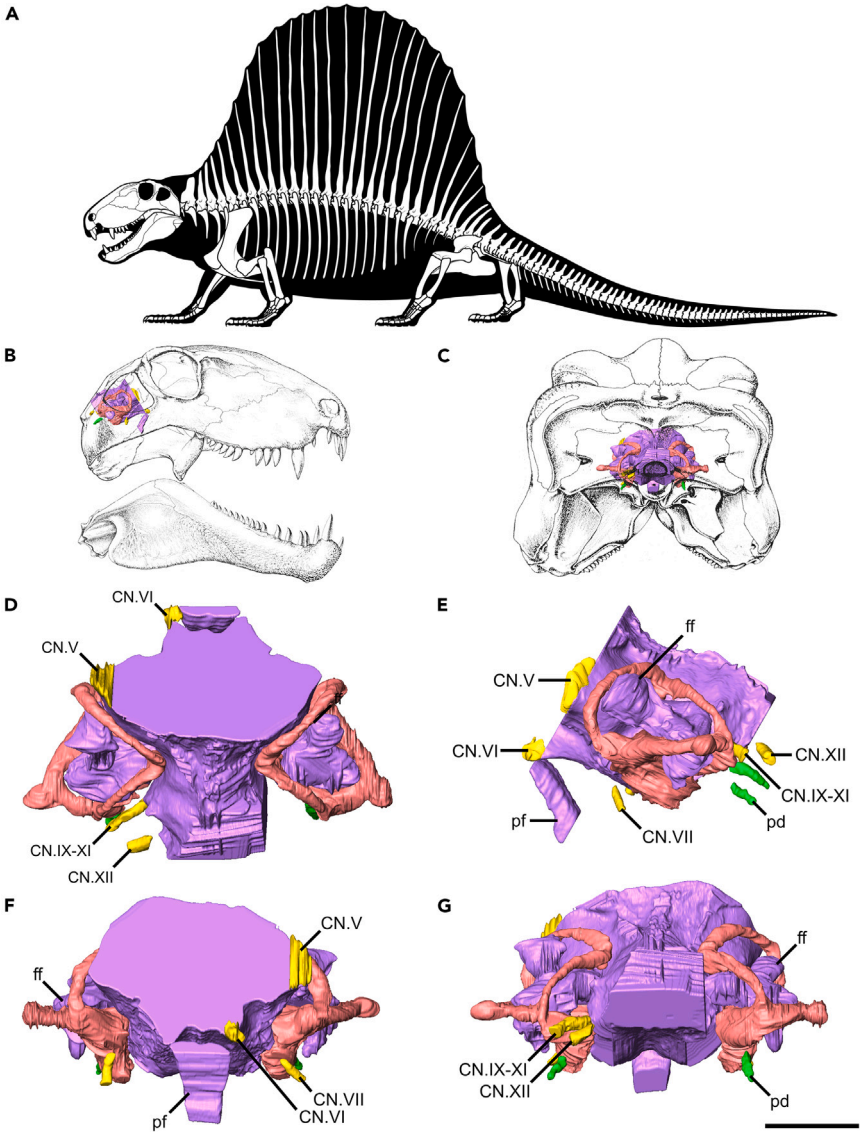

Figure 2. *Dimetrodon* endocasts

(A) Skeletal reconstruction of *Dimetrodon*.

(B and C) Endocast in skull in (B) right, (C) occipital views.

(D–G) Endocast in (D) dorsal, (E) left, (F) anterior, (G) posterior views. Scale bar equals 1 cm. Views A-C not to scale.

RESULTS

Description

Brain

As it is only the posterior portion of the braincase that is preserved in FMNH UC 423, our reconstruction of the brain of *Dimetrodon* only extends as far anteriorly as the pituitary fossa. The contours of the different brain regions are ambiguous, indicating a relatively poor fit between the brain and the surrounding hard tissues, but the general shape is apparent (Figure 2). The medulla oblongata is mediolaterally broad and there is a pronounced pontine flexure of approximately 43°; the region of the cephalic flexure is not preserved.

A large recess, identified here as a floccular fossa, occupies much of the periotic region (Figure 2). The fossa extends anteroposteriorly to span the space between the anterior and posterior semicircular canals, ventrally to the dorsoventral midpoint of the vestibule, and almost completely fills the space defined by

the lateral semicircular canal. The fossa identified here as housing the flocculus was suggested by Romer and Price[14] to have been associated with the perilymphatic system, while Hopson[22] identified a blunt swelling anterior to the inner ear as a putative flocculus. The identification of the structure described here as a floccular fossa is the most likely, as the fossa that houses the flocculus in modern tetrapods is always located within the space defined by the anterior semicircular canal,[9,31–33] as is seen in *Dimetrodon*, and structures of similar shape within the same region have been identified as floccular fossae in other taxa.[11,33,34] However, the possibility of a perilymphatic contribution to at least some portion of this fossa cannot be completely excluded; see discussion section for further detail.

The pituitary extends directly ventrally, terminating at the level of the ventral most extent of the vestibule (Figures 2E and 2F). Previous descriptions of the pituitary of *Dimetrodon* have disagreed on the morphology of the structure. Case[20,21] describes the pituitary as extending far posteriorly into the body of the basisphenoid, while Hopson[22] describes it as a vertical, narrow, elongated structure with no posterior extension. The large vacuity within the basisphenoid identified by Case[20,21] is indeed present, but it is unlikely to represent a posterior expansion of the pituitary, as the space expands posterolaterally through the basisphenoid to seemingly open into the wide canal connecting the vestibule to the fenestra vestibuli.

Innervations

The trigeminal nerve (CN.V) is the largest of the cranial nerves, exiting the brain directly medial to the ampulla of the anterior semicircular canal (Figure 2). The abducens nerve (CN.VI) passes directly anteriorly through the dorsum sellae, just lateral to the pituitary stalk. The facial nerve (CN.VII) originates anterior to the vestibule and passes posterolaterally to exit the braincase anterior to the fenestra vestibuli. An opening for an endolymphatic duct was identified by Romer and Price[14] posterodorsal to the facial nerve, but no such path could be identified in FMNH UC 423. The metotic foramen (CN.IX-XI) is only slightly larger than the foramen for the hypoglossal nerve (CN.XII), which is relatively large. An anteroposteriorly directed canal, tentatively identified as the perilymphatic duct, exits the vestibule at the level of the secondary common crus and exits the braincase through the posterior surface of the opisthotic. The paths of the internal carotids could not be discerned in the CT data.

Endosseous labyrinth

The bony labyrinth of *Dimetrodon* is surprisingly well ossified with the paths of all canals, and the margins of the vestibule clearly traceable (Figures 1 and 2). The internal auditory meatus is widely open, but to a lesser degree than has been described previously,[1] such that the medial wall of the vestibule and the ventral portion of the common crus is the only region of the inner ear that is not fully enclosed. The sutures between the supraoccipital, prootic, and opisthotic could not be discerned in the CT data, such that the relative contributions of each element to the housing of the bony labyrinth cannot be commented upon here.

Only the dorsal most portion of the common crus is preserved, but the greater dorsoventral height of the anterior semicircular canal (ASC) relative to the posterior canal indicates that the common crus are slightly caudally tilted (Figure 3). The ASC is the longest and shows the largest radius of curvature. The posterior (PSC) and lateral (LSC) canals are sub equal in length and show roughly similar radii, with the radius of curvature of the PSC being marginally smaller than that of the LSC. The ASC is arcuate along its entire length, while the PSC is nearly straight in its midportion and is slightly anterodorsally bowed. The LSC is the most strongly curved of the canals and is only moderately elliptical, while the vertical canals are strongly elliptical, with the PSC showing slightly more ellipticity than the ASC. The angles between the ASC and PSC and between the ASC and LSC are nearly orthogonal at 85° and 88° respectively, while the angle between the LSC and PSC are more acute, although only by approximately 10°. All three canals are moderately to strongly elliptical, with the LSC being the least (ellipticity of 0.49) and the PSC is the most elliptical (ellipticity of 0.84). All measurements are given in Table 1.

All the ampullae are prominent (Figure 3). The PSC and LSC join in the secondary common crus; within this structure, the PSC passes posteroventrally to the LSC to enter the vestibule directly ventral to the entrance of the LSC. A relatively large, nubbin-like protrusion can be seen on the lateral surface of the LSC, just before it curves medially to meet with the PSC in the secondary common crus. It is unlikely that this structure has a functional role, as a genuine protrusion off or diversion of the path of any semicircular canal would impact the flow of endolymph and thus impede the sensitivity of that canal. This protrusion is most likely an artifact related to the ossification patterns of the endocranium.

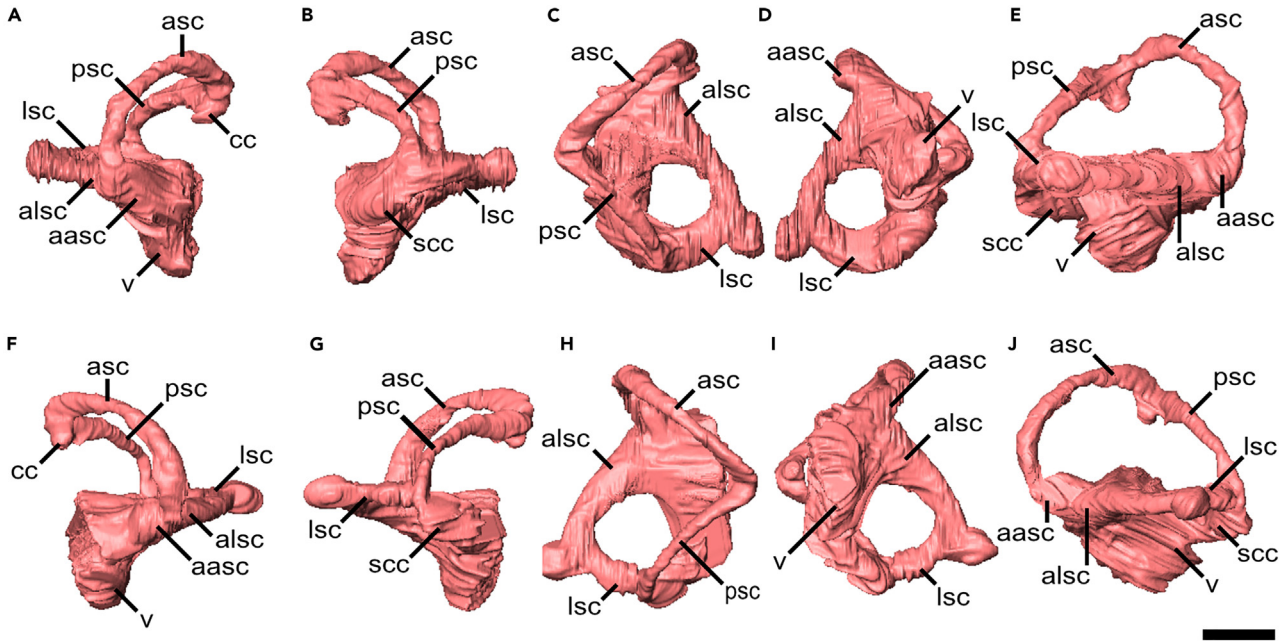

Figure 3. Virtual endocasts of the inner ear of *Dimetrodon*

(A–E) right labyrinth and (F–J) left labyrinth in (A and F) anterior, (B and G), posterior, (C and H) dorsal, (D and I) ventral, and (E and J) lateral views. Scale bar equals 5 mm.

The vestibule is short and rounded, forming an anteroposterior oval in ventral view (Figures 3D and 3I). No distinct cochlear recess could be identified. A relatively wide canal connects the vestibule to the fenestra vestibuli. The hearing frequency range and mean best hearing frequency were estimated from the length of the vestibule with estimated values of approximately 2500 Hz and 1500 Hz, respectively (Table 1).

Ancestral state reconstructions

A moderate brain flexure of approximately 50° is reconstructed as ancestral both for Therapsida, aligning with the condition seen in *Dimetrodon*, and for Synapsida as a whole (Figure 4A). Both the ML and MP analyses overwhelmingly support the presence of large floccular fossae (Figures 4B and 5B) and short, broad secondary common crus (Figures 4C and 5C) at the root of the synapsid clade. A distinct cochlear recess is reconstructed by the ML analysis at the ancestral condition throughout synapsids (Figure 4D). In contrast, the MP analysis reconstructs the absence of a cochlear recess as ancestral below dicynodonts (Figure 5D).

DISCUSSION

Comparisons with other Paleozoic amniotes

Comparative interpretations of our findings with other pelycosaur-grade synapsids are restricted by a general lack of endocast data and are by necessity limited to varanopids and therapsids, but nonetheless provide considerable new insights into the paleobiology of this early apex predator. A simplified phylogeny showing the brain and inner ear endocasts of the major clades of synapsids is given in Figure 6.

Endocast

Overall, the endocast of *Dimetrodon* is largely plesiomorphic than that of more derived synapsids, with no expansion of the cerebellum and no direct imprint of the brain or surrounding organs on the endocast, suggesting a relatively poor fit between the brain and the braincase. The strong pontine flexure is similar to that described in the biarmosuchians and dicynodonts,[6,32] differing from the more linear morphology seen in the varanopids and most other non-mammalian therapsids.[8,9,11,31,40] Brain flexures are known to vary substantially across taxa with an apparent trend toward stronger flexures in smaller taxa.[41,42] The relationship between overall body size and degree of brain flexure results from the negative allometric relationship between brain and body size, wherein smaller taxa tend to possess relatively larger brains that

Table 1. Measurements of the bony labyrinth and estimation of the hearing range and mean best hearing frequency of *Dimetrodon*

	Left	Right	Average
Basicranial length (mm)	–	–	29.82
Vestibule length (mm)	5.48	5.44	5.46
ASC height (mm)	6.93	7.98	7.46
ASC width (mm)	9.63	9.21	9.42
ASC length (mm)	20.36	19.64	20.00
ASC radius of curvature (mm)	4.14	4.30	4.22
ASC eccentricity	0.80	0.79	0.79
PSC height (mm)	5.39	5.18	5.29
PSC width (mm)	8.03	7.95	7.99
PSC length (mm)	18.02	15.68	16.85
PSC radius of curvature (mm)	3.36	3.28	3.32
PSC eccentricity	0.84	0.84	0.84
LSC height (mm)	7.37	6.21	6.79
LSC width (mm)	7.51	7.50	7.51
LSC length (mm)	18.62	16.75	17.69
LSC radius of curvature (mm)	3.72	3.43	3.57
LSC eccentricity	0.47	0.52	0.49
Hearing range (Hz)	2484.10	2464.68	2474.39
Mean best hearing frequency (Hz)	1564.59	1554.05	1559.32
∠ ASC-PSC (°)	83.2	88.6	85.90
∠ ASC-LSC (°)	88.4	88.2	88.3
∠ PSC-LSC (°)	76.6	79.9	78.25

Eccentricity values closer to 1 indicate greater ellipticity (more oval), while values closer to 0 indicate greater circularity.

are thus more constrained by the small size of the surrounding skull and the additional spatial constraints imposed by the other structures that must be contained within a skull, including the eyes.[42] This trend is not universal; however, as differences in overall skull shape can override the influence of size.[42] As FMNH UC 423 likely represents a relatively small taxon of *Dimetrodon*, it is possible that the flexure seen here relates to the small size of the animal; however, due to the absence of other associated materials from the specimen, and the lack of endocast data for other species of *Dimetrodon*, the presence or nature of any relationship between body size and cranial flexure in this genus is uncertain.

The floccular fossa in *Dimetrodon* is similar in shape and relative size to that of the varanopids;[11] in more derived synapsids the structure is typically more rounded and lacks the posterior and ventral extensions seen in the varanopids and *Dimetrodon*.[9,31,32] The Early Triassic cynodont *Galesaurus* also displays a strongly protruding floccular fossa more similar to that in *Dimetrodon* but, like other therapsids, lacks the aforementioned extensions.[35] Romer and Price[14] noted the recess identified here as a floccular fossa and suggested that its unusual morphology indicates a perilymphatic function. The structure described here is most likely at least partly floccular, as only the flocculus is known to extend into the space defined by the anterior semicircular canal,[9,31–33] and structures within the same region are almost universally identified as floccular fossae in other taxa.[11,33,34] However, given the dramatic difference in morphology shown here compared to that of therapsids, a perilymphatic function for some portion of the large fossa described in both *Dimetrodon* and the varanopids cannot be excluded. If part of this region is perilymphatic, the significance of its expansion in the region of the floccular fossa would have no equivalent in modern tetrapods.

Even if the posterior and ventral extensions of the fossa are in fact perilymphatic, the definitively floccular portion of the fossa remains quite large. The large size of the floccular fossa in *Dimetrodon* is potentially indicative of adaptations for rapid head movements;[34] as the flocculus in extant taxa is heavily involved in gaze stabilization and reflex control of the neck, enlarged floccular fossae have often been interpreted

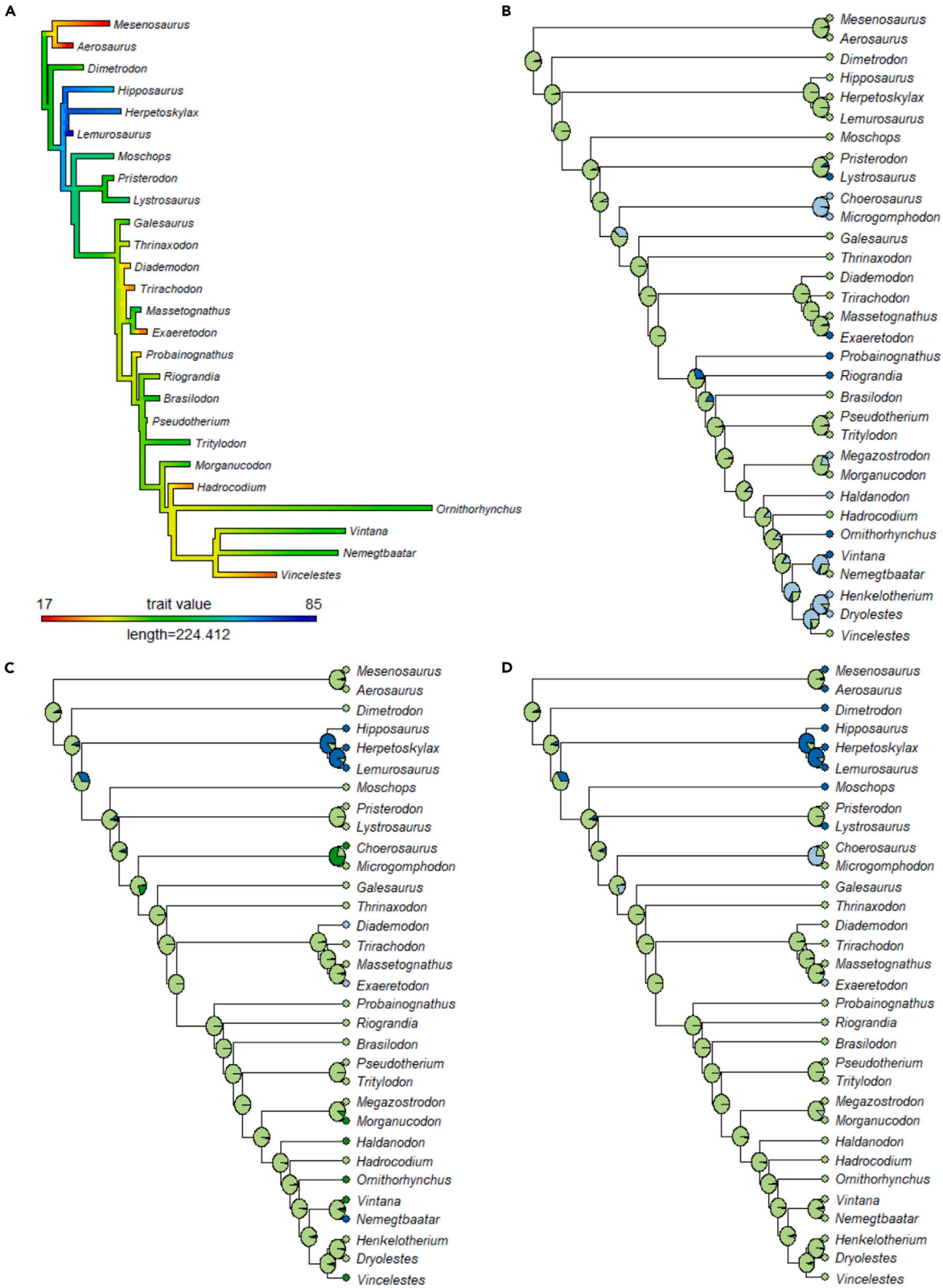
A
Mesenosaurus
Aerosaurus
Dimetrodon
Hipposaurus
Herpetoskylax
Lemurosaurus
Moschops
Pristerodon
Lystrosaurus
Galesaurus
Thrinaxodon
Diademodon
Trirachodon
Massetognathus
Exaeretodon
Probainognathus
Riograndia
Brasilodon
Pseudotherium
Tritylodon
Morganucodon
Hadrocodium
Ornithorhynchus
Vintana
Nemegtbaatar
Vincelestes
17
trait value
85
length=224.412
B
Mesenosaurus
Aerosaurus
Dimetrodon
Hipposaurus
Herpetoskylax
Lemurosaurus
Moschops
Pristerodon
Lystrosaurus
Choerosaurus
Microgomphodon
Galesaurus
Thrinaxodon
Diademodon
Trirachodon
Massetognathus
Exaeretodon
Probainognathus
Riograndia
Brasilodon
Pseudotherium
Tritylodon
Megazostrodon
Morganucodon
Haldanodon
Hadrocodium
Ornithorhynchus
Vintana
Nemegtbaatar
Henkelotherium
Dryolestes
Vincelestes
C
Mesenosaurus
Aerosaurus
Dimetrodon
Hipposaurus
Herpetoskylax
Lemurosaurus
Moschops
Pristerodon
Lystrosaurus
Choerosaurus
Microgomphodon
Galesaurus
Thrinaxodon
Diademodon
Trirachodon
Massetognathus
Exaeretodon
Probainognathus
Riograndia
Brasilodon
Pseudotherium
Tritylodon
Megazostrodon
Morganucodon
Haldanodon
Hadrocodium
Ornithorhynchus
Vintana
Nemegtbaatar
Henkelotherium
Dryolestes
Vincelestes
D
Mesenosaurus
Aerosaurus
Dimetrodon
Hipposaurus
Herpetoskylax
Lemurosaurus
Moschops
Pristerodon
Lystrosaurus
Choerosaurus
Microgomphodon
Galesaurus
Thrinaxodon
Diademodon
Trirachodon
Massetognathus
Exaeretodon
Probainognathus
Riograndia
Brasilodon
Pseudotherium
Tritylodon
Megazostrodon
Morganucodon
Haldanodon
Hadrocodium
Ornithorhynchus
Vintana
Nemegtbaatar
Henkelotherium
Dryolestes
Vincelestes

Figure 4. Ancestral state reconstructions for four key neuroanatomical traits conducted via maximum likelihood

(A) Brain flexure, with character states ranging from 17° to 85°.

(B) Flocculus size, with character states of either a small bump extending just into the area bounded by the ASC (state 0; dark blue) or a large protrusion extending far past the ASC (state 1; light green).

(C) Secondary common crus, with character states of absent (state 0; dark blue), short and broad (state 1; light green), or elongate and narrow (state 2; dark green).

(D) Cochlea, with character states of absent (state 0; dark blue) or present (state 1; light green). In all reconstructions, light blue represents taxa for which a given trait could not be coded.

as indicative of a high degree of head-eye coordination.[33,43–45] However, the relationship of floccular fossa size with ecological or behavioral factors is not universally agreed upon. Work by Ferreira-Cardoso et al.[46] found no significant relationships between floccular fossa size and agility, locomotor style, feeding strategy, or activity patterns in either extant mammals or birds. Earlier work by Walsh et al.[44] similarly found no relationship between the size of the floccular fossa and flying ability in birds. Further, identification of fossae such as these in fossil taxa as floccular fossae is problematic, as this fossa is known to house different neural tissues in various extant clades and the size relationship between the flocculus itself and the fossa in which it resides is not precise, thus hindering analyses of floccular size in extinct vertebrates.[34,46] Conclusions regarding the function of the flocculus in *Dimetrodon* would be aided by comparison with closely related herbivorous taxa such as the edaphosaurs or caseasaurs, but such comparisons are precluded by a lack of published data; Case[47] provided a description of the inner ear of *Edaphosaurus* but neither described nor figured the floccular recess, and no description of the recess could be found for any caseasaur.

Canals and vestibule

The bony labyrinth of *Dimetrodon* is very similar in overall shape to that of the varanopids.[11] While the common crus could not be extracted in its entirety in *Dimetrodon*, the paths of all three canals are nearly identical to the varanopids in all views.[11] The dorsal expansion of the anterior canal relative to the posterior canal is much less pronounced in *Dimetrodon* than in the gorgonopsians, dinocephalians, or the dicynodont *Pristerodon*,[8,9,31] being more similar to the condition in the varanopids and the dicynodont *Niassodon*.[11,32] The strong ellipticity is also most similar to that of the varanopids and dicynodonts, contrasting strongly with the circular canals of mammals.[11,26,48]

Along with the near-orthogonality of the canal system in *Dimetrodon*, the high ellipticity may indicate specialization for rapid head movements, aligning with the hypothesized active predatory lifestyle of *Dimetrodon*; however, the degree of relationship between ellipticity, orthogonality, and canal sensitivity is debated.[48,49] If the ellipticity seen in *Dimetrodon* is indeed related to the rapid head movements involved in predation, herbivorous taxa such as *Edaphosaurus* would be expected to display less ellipticity. Case[47] provides a description of the inner ear of *Edaphosaurus*; in contrast to the expected low degree of ellipticity, the semicircular canals figured by Case appear to be at least moderately elliptical, but the lack of any measurements of the canal system in *Edaphosaurus* preclude a more precise determination of ellipticity.

The short, rounded vestibule seen in *Dimetrodon* is similar to that of the varanopids,[11] contrasting with the more conical condition seen in most of the more derived synapsids.[7–9,31,32,40] Unlike the varanopids, in which the fenestra vestibuli directly contacts the posteroventral most portion of the vestibule,[11] the fenestra vestibuli in *Dimetrodon* is more similar to some biarmosuchians in being situated at the end of a long canal.[7] However, while this canal is thin and extends through the basicranium in the biarmosuchians,[7] in *Dimetrodon* it is widely open.

Functional implications

Vestibule length has been shown to correlate with hearing sensitivity in a wide array of tetrapods, with relatively longer vestibules (scaled to basicranial axis length) being associated with sensitivity to higher frequencies.[27] Sensitivity estimates for a range of non-mammalian therapsids were provided by Benoit et al.[7]; however, these initial estimates were calculated using data that were not log-transformed, resulting in estimated sensitivities in the range of extant mammals and birds. Re-calculated estimates for selected taxa using log-transformed data, as per the method of Walsh et al.,[27] are provided in Table 2. The

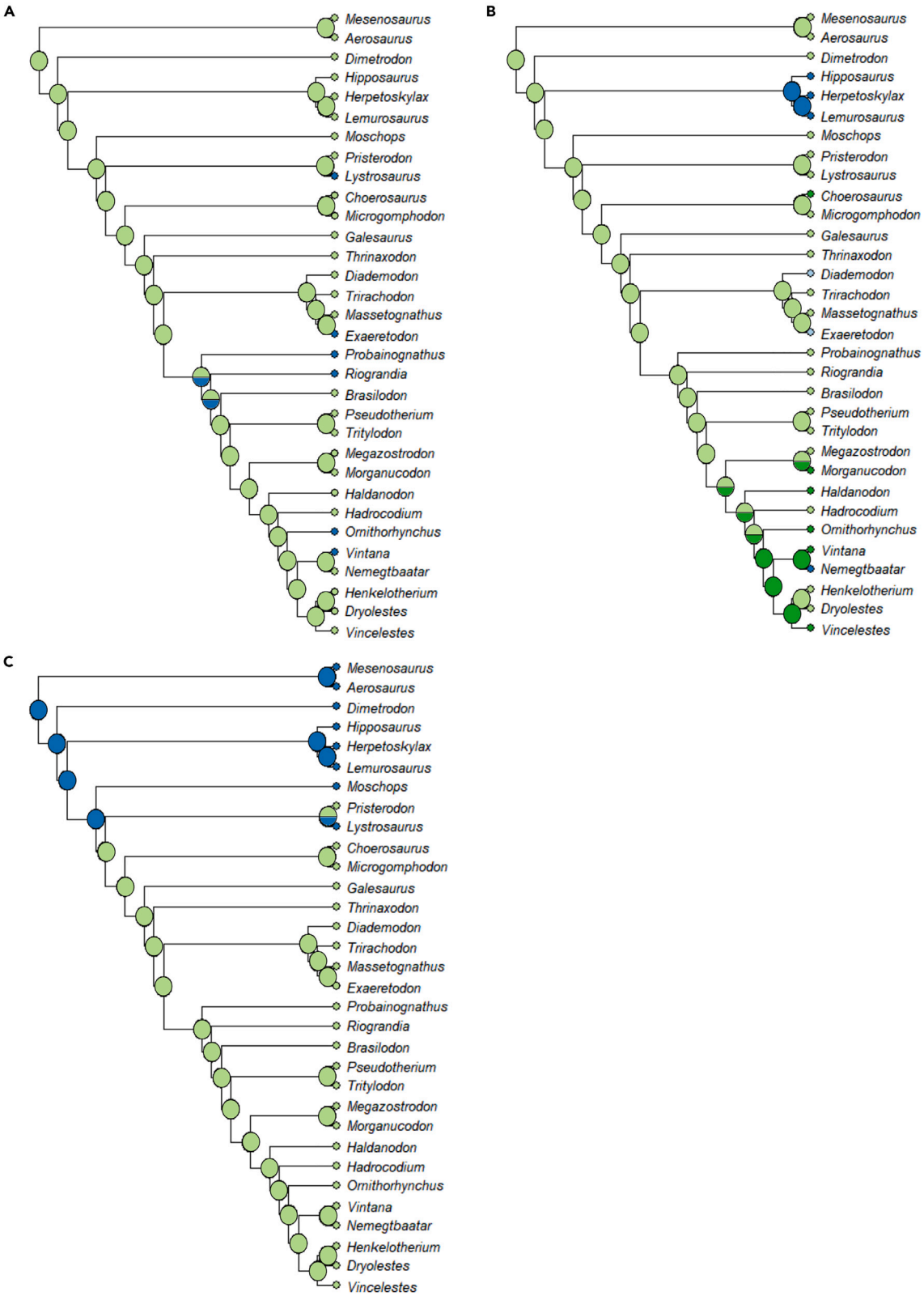
A
Mesenosaurus
Aerosaurus
Dimetrodon
Hipposaurus
Herpetoskylax
Lemurosaurus
Moschops
Pristerodon
Lystrosaurus
Choerosaurus
Microgomphodon
Galesaurus
Thrinaxodon
Diademodon
Trirachodon
Massetognathus
Exaeretodon
Probainognathus
Riograndia
Brasilodon
Pseudotherium
Tritylodon
Megazostrodon
Morganucodon
Haldanodon
Hadrocodium
Ornithorhynchus
Vintana
Nemegtbaatar
Henkelotherium
Dryolestes
Vincelestes
B
Mesenosaurus
Aerosaurus
Dimetrodon
Hipposaurus
Herpetoskylax
Lemurosaurus
Moschops
Pristerodon
Lystrosaurus
Choerosaurus
Microgomphodon
Galesaurus
Thrinaxodon
Diademodon
Trirachodon
Massetognathus
Exaeretodon
Probainognathus
Riograndia
Brasilodon
Pseudotherium
Tritylodon
Megazostrodon
Morganucodon
Haldanodon
Hadrocodium
Ornithorhynchus
Vintana
Nemegtbaatar
Henkelotherium
Dryolestes
Vincelestes
C
Mesenosaurus
Aerosaurus
Dimetrodon
Hipposaurus
Herpetoskylax
Lemurosaurus
Moschops
Pristerodon
Lystrosaurus
Choerosaurus
Microgomphodon
Galesaurus
Thrinaxodon
Diademodon
Trirachodon
Massetognathus
Exaeretodon
Probainognathus
Riograndia
Brasilodon
Pseudotherium
Tritylodon
Megazostrodon
Morganucodon
Haldanodon
Hadrocodium
Ornithorhynchus
Vintana
Nemegtbaatar
Henkelotherium
Dryolestes
Vincelestes

Figure 5. Ancestral state reconstructions for flocculus size, secondary common crus morphology, and cochlear recess under a maximum parsimony framework

(A) Flocculus size, with character states of either a small bump extending just into the area bounded by the ASC (state 0; light green) or a large protrusion extending far past the ASC (state 1; dark blue).

(B) Secondary common crus, with character states of absent (state 0; dark blue), short and broad (state 1; light green), or elongate and narrow (state 2; dark green).

(C) Cochlea, with character states of absent (state 0; dark blue) or present (state 1; light green).

estimated hearing range and mean best hearing frequency (2500 Hz and 1500 Hz, respectively) in *Dimetrodon* are similar to those for varanopids and most other non-mammalian synapsids.[7,11]

Previous estimates of the auditory abilities of *Dimetrodon*, based solely on the massive size of the stapes and the lack of a tympanic membrane, suggested sensitivity to only very low frequencies, below 1000 Hz.[1] While the estimates given here for *Dimetrodon* are indeed very low relative to extant synapsids, they are slightly higher than the original estimate by Allin and Hopson[1] and are similar to or higher than those of many extant sauropsids[27,50–53] excluding birds.[54,55] Interestingly, the estimates for *Dimetrodon* are higher than some taxa for whom some degree of air-borne hearing is known, including some geckos and skinks,[50] suggesting strongly that *Dimetrodon* was sensitive to a greater range of frequencies beyond the ultra-low-frequency ground-borne sounds previously anticipated, and may have been important in prey acquisition. The sphenacodontids are the first synapsids to possess a reflected lamina of the angular, which would come to play a critical role in the evolution of the mammalian ear[3]; thus, clarifying the auditory capabilities of *Dimetrodon* is essential for accurately contextualizing the evolutionary changes leading to hearing in crown mammals.

The presence of a probable perilymphatic duct further complicates the question of sphenacodontid audition; perilymphatic ducts plesiomorphically serve to drain the perilymph from the inner ear in amniotes but are often co-opted to function within impedance matching hearing systems in reptiles.[56] Such systems are typically associated with gracile moving stapes that are actuated by a relatively larger tympanic membrane, and with stapedial footplates[57] that are smaller than the fenestra vestibuli where they are attached. Due to the forces created within the inner ear by the actuation of the fenestra vestibuli by movement of the stapes, impedance matching hearing systems require a pressure-release mechanism.[58] This pressure release can be achieved by a fenestra rotunda as in crown mammals or a perilymphatic sac or duct as in many diapsids.[39,56,59] Ducts similar or identical to that found in *Dimetrodon* have been identified as perilymphatic ducts across amniotes, including archosaurs and archosauromorphs,[42,60] squamates,[61] and mammaliaforms.[39] In *Dimetrodon*; however, the stapes is massive, contacts the rim of the fenestra vestibuli, and attaches to the paroccipital process of the opisthotic via a large dorsal process, and thus likely served a bracing function to support the braincase within the skull.[14] Given the clearly non-tympanic role of the stapes in *Dimetrodon* and the probable absence of an air-filled middle ear, it is currently unclear what functions a pressure release mechanism such as a perilymphatic duct would serve.

One possibility deserving of further exploration is the potential for the auditory system of *Dimetrodon* to represent a very early stage in the evolution of the mammalian impedance-matching ear, with the reflected lamina of the angular acting as an incipient tympanum in coordination with the overlying musculature. This possible function was initially proposed in therapsids by Allin[3] and, should the lamina have served a sound-receiving function in these more derived synapsids, it is not unreasonable to expect a similar function in *Dimetrodon*. The mechanisms by which the lamina could have performed such a function in therapsids have been discussed by Olroyd and Sidor,[62] with the deepening of the angular cleft allowing the lamina to vibrate more freely and the topography of the lamina serving to modify its vibrational qualities. Alternatively, the reflected lamina may have served to support a true tympanic membrane, if one was present (see Kemp[19] for a review of the arguments for and against the presence of a postquadrate tympanum in sphenacodontids). However, under either hypothesized function for the reflected lamina, we would expect to see an increase, however slight, in sensitivity to higher frequency sounds relative to taxa lacking this structure. Comparison of the estimated hearing sensitivity values for *Dimetrodon* and several therapsid taxa (Tables 1 and 2) with those of varanopids, the only synapsids without a reflected lamina for which hearing sensitivity estimates are currently available, shows no apparent difference in hearing range or mean best hearing frequency.[11] The lack of sensitivity estimates for other pelycosaur-grade synapsids that do not possess reflected laminae precludes any definitive determination of the impact of the reflected lamina on hearing sensitivity, but the data currently available do not support the hypothesis of a tympanic function for the reflected lamina of the angular.

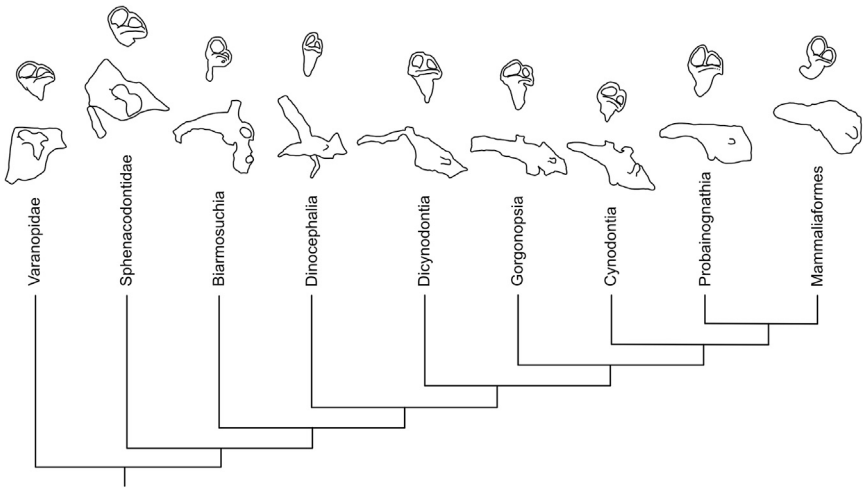

Figure 6. Simplified phylogeny of some of the major clades of synapsids, with representative endocasts for each clade

Clades are represented as follows: Varanopidae by an indeterminate mycterosaurine[11]; Sphenacodontidae by *Dimetrodon*; Biarmosuchia by *Lemurosaurus*[6]; Dinocephalia by *Moschops*[6]; Dicynodontia by *Niassodon*[28]; Gorgonopsia by an indeterminate gorgonopsian[27]; Cynodontia by *Galesaurus*[35]; Probainognathia by *Riograndia*[36,37] (cranial endocast) and *Pseudotherium*[38] (inner ear endocast); Mammaliaformes by *Morganucodon*.[2,39] Endocasts are not to scale.

A perilymphatic duct exiting the otic capsule via a distinct foramen and invading the metotic foramen has been suggested to be the plesiomorphic condition for amniotes.[63] This is supported by the presence of perilymphatic ducts in an array of extinct and extant members of both the sauropsid and synapsid lineages.[39,56,59,64] However, there are a number of taxa for which there are no indications of a distinct perilymphatic duct, including captorhinids[65] and the basal diapsid *Youngina*.[56] If the presence of a perilymphatic duct is in fact plesiomorphic for amniotes, two issues are raised. First, perilymphatic ducts must have initially served other functions unrelated to hearing and were only later co-opted for pressure release as impedance matching hearing systems evolved in amniotes. Second, the criteria for identifying perilymphatic ducts may be inadequate, as current definitions must be failing to capture the ducts present in amniotes such as the captorhinids and *Youngina*.

Ancestral state reconstruction

In six of the seven reconstructions, the reconstructed ancestral state for therapsids aligns with the condition seen here in *Dimetrodon*, thereby supporting the long-standing practice of viewing *Dimetrodon* as broadly representative of the ancestral therapsid condition. A moderate brain flexure, similar to that seen in the crown mammals *Vintana*, *Nemegtbaatar*, and *Ornithorhynchus* is reconstructed as ancestral for both Synapsida and Therapsida and appears throughout the phylogeny. This suggests that, contrary to previous assumptions that a tubular, unflexed brain represented the plesiomorphic state for synapsids,[11,31,40] both the strongly flexed brains seen in biarmosuchians and the more tubular brains of varanopids and *Vincelestes* may instead represent derived conditions relative to an ancestrally moderately flexed state. The analyses of floccular fossa size and secondary common crus morphology overwhelmingly support a large flocculus and short, broad secondary common crus as ancestral for synapsids under both the ML and MP frameworks, aligning with the morphologies described here in *Dimetrodon* and by Bazzana et al.[11] in the varanopids.

The only significant disagreement between the results of the ML and MP analyses are in the cochlear recess reconstructions, with the MP analysis supporting the absence of a recess stemward of dicynodonts while the ML strongly supports a distinct recess as ancestrally present even for those taxa for which no cochlear recess exists. This result underscores the importance of using fossil data to validate the results of backward-projecting analyses like ASR. Given the presence of distinct cochlear recesses in the vast majority of fossil synapsids, if we did not have endocast data for cochlea-lacking taxa such as the pelycosaurs or biarmosuchians, we would erroneously assume that cochleae were present in the ancestor of all synapsids. While incorrectly attributing a character state to a taxon may seem superficially to be a minor issue, an error

Table 2. Estimates of hearing range and mean best hearing frequency of selected synapsid taxa

Taxon	Clade	Hearing range (Hz)	Best hearing frequency (Hz)
Lemurosaurus	Biarmosuchia	2580.68	1616.98
Hipposaurus	Biarmosuchia	1745.68	1164.03
Moschops	Dinocephalia	2776.94	1723.44
Patronomodon	Anomodontia	3786.09	2270.86
Eodicynodon	Dicynodontia	2868.19	1772.94
Pristerodon	Dicynodontia	3606.42	2173.39
Scylacocephalus	Gorgonopsia	3003.67	1846.43
Choerosaurus	Therocephalia	1441.31	998.92
Euchambersia	Therocephalia	2354.92	1494.51
Cynosaurus	Cynodontia	1550.49	1058.15
Galesaurus	Cynodontia	2041.34	1324.41
Trirachodon	Cynognathia	2483.85	1564.45
Lumkuia	Probainognathia	1556.92	1061.63
Megazostrodon	Mammaliaformes	4879.48	2863.97

Estimates re-calculated using the vestibular length and basicranial axis length measurements provided by Benoit et al. (2017b).[7]

such as this could have significant ramifications for our understanding of inner ear evolution in amniotes as a whole. Taken in isolation, the reconstruction provided by the ML analysis would suggest that distinct cochlear recesses could have been present in the very earliest amniotes, or even in the ancestor of amniotes, which would in turn imply a homology between the expanded cochleae of synapsids and sauropsids, something which is known to be incorrect from examination of early members of both lineages.[11,66,67] It is only with the examination of the fossils themselves that the results of any reconstruction can be validated or accurately contextualized.

This first computed tomographic study of the brain and bony labyrinth of the iconic synapsid *Dimetrodon* reveals previously unrecognized aspects of sphenacodontid neuroanatomy that shed new light on its palaeobiology and the evolution of the mammalian inner ear. Our findings extend our understanding of synapsid palaeoneuroanatomy to one of the most widely recognizable early synapsids and early terrestrial apex predators, and indicate a much greater diversity in the sensory function of pelycosaur-grade synapsids than previously anticipated. As the sister group to Therapsida, the sphenacodontid neuroanatomy and sensory function revealed here help to define the plesiomorphic condition for therapsids as a whole and clarify the foundation upon which the defining features of mammals eventually arose. ASR indicate that the neuroanatomy of *Dimetrodon* is generally representative of the ancestral condition for therapsids, and likely for the broader synapsid condition, while also underscoring the importance of validating any reconstructive analysis with empirical fossil data.

Limitations of the study

Our results are based on a single endocast virtually extracted from an isolated braincase; as a result, our interpretations lack the broader context provided by larger sample sizes, and it is unclear whether the features identified in *Dimetrodon* are shared by other sphenacodontids. In addition, our ancestral state reconstruction is limited by the relative paucity of endocast data on fossil synapsids. While the number of non-mammalian synapsids to receive neuroanatomical descriptions has greatly increased in recent years, the endocasts of the vast majority of fossil synapsids remain to be studied, and the information gained from such taxa could change the reconstructions and the resultant interpretations of synapsid neuroevolution.

STAR★METHODS

Detailed methods are provided in the online version of this paper and include the following:

- KEY RESOURCES TABLE
- RESOURCE AVAILABILITY

SUPPLEMENTAL INFORMATION

Supplemental information can be found online at https://doi.org/10.1016/j.isci.2023.106473.

ACKNOWLEDGMENTS

Thanks to Ken Angielczyk for data access, Danielle Dufault for the skeletal reconstruction in Figure 2, and Mary Silcox for discussions. Thanks to the comments of the anonymous reviewers of an earlier version of this manuscript, whose feedback greatly improved the overall work. This research was supported by NSERC grants to D.C.E.(RGPIN-2018-06788) and R.R.R.(RGPIN-2020-04959) and an NSERC scholarship to K.B.A.

AUTHOR CONTRIBUTIONS

K.B.A., D.C.E., and R.R.R. conceived the study; K.B.A. collected and analyzed the data; K.B.A. wrote the paper with the input of D.C.E. and R.R.R. All authors approved the submitted version.

DECLARATION OF INTERESTS

The authors declare no competing interests.

Received: October 25, 2022
Revised: February 16, 2023
Accepted: March 19, 2023
Published: March 21, 2023

REFERENCES

1. Allin, E.F., and Hopson, J.A. (1992). Evolution of the auditory system in Synapsida ("mammal-like reptiles" and primitive mammals) as seen in the fossil record. In The Evolutionary Biology of Hearing, D.B. Webster, R.R. Fay, and P. AN, eds. (New York: Springer), pp. 587–614. https://doi.org/10.1007/978-1-4612-2784-7_37.

2. Rowe, T.B., Macrini, T.E., and Luo, Z.-X. (2011). Fossil evidence on origin of the mammalian brain. Science *332*, 955–957. https://doi.org/10.1126/science.1203117.

3. Allin, E.F. (1975). Evolution of the mammalian middle ear. J. Morphol. *147*, 403–437. https://doi.org/10.1002/jmor.1051470404.

4. Barton, R.A., and Harvey, P.H. (2000). Mosaic evolution of brain structure in mammals. Nature *405*, 1055–1058. https://doi.org/10.1038/35016580.

5. Luo, Z.-X. (2001). The inner ear and its bony housing in tritylodontids and implications for evolution of the mammalian ear. Bull. Mus. Comp. Zool. *156*, 81–97.

6. Benoit, J., Fernandez, V., Manger, P.R., and Rubidge, B.S. (2017). Endocranial casts of pre-mammalian therapsids reveal an unexpected neurological diversity at the deep evolutionary root of mammals. Brain Behav. Evol. *90*, 311–333. https://doi.org/10.1159/000481525.

7. Benoit, J., Manger, P.R., Fernandez, V., and Rubidge, B.S. (2017). The bony labyrinth of late Permian Biarmosuchia: palaeobiology and diversity in non-mammalian Therapsida. Palaeontol. Afr. *52*, 58–77.

8. Benoit, J., Manger, P.R., Norton, L., Fernandez, V., and Rubidge, B.S. (2017). Synchrotron scanning reveals the palaeoneurology of the head-butting *Moschops capensis* (Therapsida, Dinocephalia). PeerJ *5*, e3496. https://doi.org/10.7717/peerj.3496.

9. Laaß, M. (2015). Virtual reconstruction and description of the cranial endocast of *Pristerodon mackayi* (Therapsida, Anomodontia). J. Morphol. *276*, 1089–1099. https://doi.org/10.1002/jmor.20397.

10. Laaß, M. (2015). Bone-conduction hearing and seismic sensitivity of the late Permian anomodont *Kawingasaurus fossilis*. J. Morphol. *276*, 121–143. https://doi.org/10.1002/jmor.20325.

11. Bazzana, K.D., Evans, D.C., Bevitt, J.J., and Reisz, R.R. (2022). Neurosensory anatomy of Varanopidae and its implications for early synapsid evolution. J. Anat. *240*, 833–849. https://doi.org/10.1111/joa.13593.

12. Benoit, J., Ford, D., Miyamae, J., and Ruf, I. (2021). Can maxillary canal morphology inform varanopid phylogenetic affinities? Acta Palaeontol. Pol. *66*, 389–393. https://doi.org/10.4202/app.00816.202.

13. Reisz, R.R. (1986). Pelycosauria. Handbuch der Paläoherpetologie, Teil 17A.

14. Romer, A.S., and Price, L.I. (1940). Review of the Pelycosauria (Geological Society of America).

15. Brink, K.S., and Reisz, R.R. (2014). Hidden dental diversity in the oldest terrestrial apex predator *Dimetrodon*. Nat. Commun. *5*, 3269. https://doi.org/10.1038/ncomms4269.

16. Barghusen, H.R. (1973). The adductor jaw musculature of *Dimetrodon* (Reptilia, Pelycosauria). J. Paleontol. *47*, 823–834.

17. Huttenlocker, A.K., Rega, E., and Sumida, S.S. (2010). Comparative anatomy and osteohistology of hyperelongate neural spines in the sphenacodontids *Sphenacodon* and *Dimetrodon* (Amniota: Synapsida). J. Morphol. *271*, 1407–1421. https://doi.org/10.1002/jmor.10876.

18. Hopson, J.A. (1966). The origin of the mammalian middle ear. Am. Zool. *6*, 437–450. https://doi.org/10.1093/icb/6.3.437.

19. Kemp, T.S. (2016). Non-mammalian synapsids: the beginning of the mammal line. In Evolution of the Vertebrate Ear – Evidence from the Fossil Record, J.A. Clack, R.R. Fay, and A.N. Popper, eds. (New York: Springer), pp. 107–137.

20. Case, E.C. (1907). Revision of the pelycosauria of North America, *55* (Carnegie Institution of Washington publication), pp. 1–176. https://doi.org/10.5962/bhl.title.45536.

21. Case, E.C. (1897). On the foramina perforating the cranial region of a Permian reptile and on a cast of its brain cavity. Am. J. Sci. *s4–3*, 321–326. https://doi.org/10.2475/ajs.s4-3.16.321.

22. Hopson, J.A. (1979). Paleoneurology. In Biology of the Reptilia 9-A, C. Gans, R.G. Northcutt, and P. Ulinsky, eds. (London: Academic Press), pp. 39–146.

23. Olson, E.C. (1938). The occipital, otic, basicranial and pterygoid regions of the Gorgonopsia. J. Morphol. *62*, 141–175. https://doi.org/10.1002/jmor.1050620202.

24. Araújo, R., David, R., Benoit, J., Lungmus, J., Spoor, F., Stoessel, A., Barrett, P., Maisano, J., Ekdale, E., Orliac, M., et al. (2022). Inner ear biomechanics reveals Late Triassic origin of mammalian endothermy. Nature *607*, 726–731. https://doi.org/10.1038/s41586-022-04963-z.

25. Reisz, R.R., Berman, D.S., and Scott, D. (1992). The cranial anatomy and relationships of *Secodontosaurus*, an unusual mammal-like reptile (Synapsida: Sphenacodontidae) from the early Permian of Texas. Zool. J. Linn. Soc. *104*, 127–184. https://doi.org/10.1111/j.1096-3642.1992.tb00920.x.

26. Goyens, J. (2019). High ellipticity reduces semi-circular canal sensitivity in squamates compared to mammals. Sci. Rep. *9*, 16428. https://doi.org/10.1038/s41598-019-52828-9.

27. Walsh, S.A., Barrett, P.M., Milner, A.C., Manley, G., and Witmer, L.M. (2009). Inner ear anatomy is a proxy for deducing auditory capability and behaviour in reptiles and birds. Proc. Biol. Sci. *276*, 1355–1360. https://doi.org/10.1098/rspb.2008.1390.

28. Paradis, E., Claude, J., and Strimmer, K. (2004). Ape : analyses of phylogenetics and evolution in R language. Bioinformatics *20*, 289–290.

29. Hellert, S., Grossnickle, D., Lloyd, G., Kammerer, C., and Angielczyk, K. Derived faunivores are the forerunners of major synapsid radiations. Preprint at Res. Sq., 10.21203/rs.3.rs-1582761/v1

30. Macrini, T.E., De Muizon, C., Cifelli, R.L., and Rowe, T. (2007). Digital cranial endocast of *Pucadelphys andinus*, a Paleocene metatherian. J. Vertebr. Paleontol. *27*, 99–107. https://doi.org/10.1671/0272-4634(2007)27.

31. Araújo, R., Fernandez, V., Polcyn, M.J., Fröbisch, J., and Martins, R.M.S. (2017). Aspects of gorgonopsian paleobiology and evolution: insights from the basicranium, occiput, osseous labyrinth, vasculature, and neuroanatomy. PeerJ *5*, e3119. https://doi.org/10.7717/peerj.3119.

32. Castanhinha, R., Araújo, R., Júnior, L.C., Angielczyk, K.D., Martins, G.G., Martins, R.M.S., Chaouiya, C., Beckmann, F., and Wilde, F. (2013). Bringing dicynodonts back to life: paleobiology and anatomy of a new emydopoid genus from the Upper Permian of Mozambique. PLoS One *8*, e80974. https://doi.org/10.1371/journal.pone.0080974.

33. Witmer, L.M., Chatterjee, S., Franzosa, J., and Rowe, T. (2003). Neuroanatomy of flying reptiles and implications for flight, posture and behavior. Nature *425*, 950–953. https://doi.org/10.1038/nature02048.

34. Schade, M., Rauhut, O.W.M., and Evers, S.W. (2020). Neuroanatomy of the spinosaurid *Irritator hallenger* (Dinosauria: Theropoda) indicates potential adaptations for piscivory. Sci. Rep. *10*, 9259. https://doi.org/10.1038/s41598-020-66261-w.

35. Pusch, L.C., Kammerer, C.F., and Fröbisch, J. (2019). Cranial anatomy of the early cynodont *Galesaurus planiceps* and the origin of mammalian endocranial characters. J. Anat. *234*, 592–621. https://doi.org/10.1111/joa.12958.

36. Rodrigues, P.G., Martinelli, A.G., Schultz, C.L., Corfe, I.J., Gill, P.G., Soares, M.B., and Rayfield, E.J. (2018). Digital cranial endocast of *Riograndia guaibensis* (Late Triassic, Brazil) sheds light on the evolution of the brain in non-mammalian cynodonts. Hist. Biol. *31*, 1195–1212. https://doi.org/10.1080/08912963.2018.1427742.

37. Kerber, L., Ferreira, J.D., Fonseca, P.H.M., Franco, A., Martinelli, A.G., Soares, M.B., and Ribeiro, A.M. (2021). An additional brain endocast of the ictidosaur *Riograndia guaibensis* (Eucynodontia: Probainognathia): intraspecific variation of endocranial traits. An. Acad. Bras. Cienc. *93*, e20200084. https://doi.org/10.1590/0001-3765202120200084.

38. Wallace, R.V.S., Martínez, R., and Rowe, T. (2019). First record of a basal mammaliamorph from the early late Triassic ischigualasto formation of Argentina. PLoS One *14*, e0218791. https://doi.org/10.1371/journal.pone.0218791.

39. Luo, Z.-X., Schultz, J.A., and Ekdale, E. (2016). Evolution of the middle and inner ears of mammaliaforms: the approach to mammals. In Evolution of the Vertebrate Ear – Evidence from the Fossil Record, J.A. Clack, R.R. Fay, and A.N. Popper, eds. (Springer New York), pp. 139–174.

40. Bendel, E.-M., Kammerer, C.F., Kardjilov, N., Fernandez, V., and Fröbisch, J. (2018). Cranial anatomy of the gorgonopsian *Cynariops robustus* based on CT-reconstruction. PLoS One *13*, e0207367. https://doi.org/10.1371/journal.pone.0207367.

41. Giffin, E.B. (1989). Pachycephalosaur paleoneurology (Archosauria: Ornithischia). J. Vertebr. Paleontol. *9*, 67–77. https://doi.org/10.1080/02724634.1989.10011739.

42. Dudgeon, T.W., Maddin, H.C., Evans, D.C., and Mallon, J.C. (2020). The internal cranial anatomy of *Champsosaurus* (Choristodera: Champsosauridae): implications for neurosensory function. Sci. Rep. *10*, 7122. https://doi.org/10.1038/s41598-020-63956-y.

43. Spoor, F., Garland, T., Krovitz, G., Ryan, T.M., Silcox, M.T., and Walker, A. (2007). The primate semicircular canal system and locomotion. Proc. Natl. Acad. Sci. USA *104*, 10808–10812. https://doi.org/10.1073/pnas.0704250104.

44. Walsh, S.A., Iwaniuk, A.N., Knoll, M.A., Bourdon, E., Barrett, P.M., Milner, A.C., Nudds, R.L., Abel, R.L., and Sterpaio, P.D. (2013). Avian cerebellar floccular fossa size is not a proxy for flying ability in birds. PLoS One *8*, e67176. https://doi.org/10.1371/journal.pone.0067176.

45. De Zeeuw, C.I., and Koekkoek, S.K. (1997). Signal processing in the C2 module of the flocculus and its role in head movement control. Prog. Brain Res. *114*, 299–320. https://doi.org/10.1016/S0079-6123(08)63371-3.

46. Ferreira-Cardoso, S., Araújo, R., Martins, N.E., Martins, G.G., Walsh, S., Martins, R.M.S., Kardjilov, N., Manke, I., Hilger, A., and Castanhinha, R. (2017). Floccular fossa size is not a reliable proxy of ecology and behaviour in vertebrates. Sci. Rep. *7*, 2005. https://doi.org/10.1038/s41598-017-01981-0.

47. Case, E.C. (1914). On the structure of the inner ear in two primitive reptiles. Biol. Bull. *27*, 213–216. https://doi.org/10.2307/1535976.

48. Araújo, R., Fernandez, V., Rabbitt, R.D., Ekdale, E.G., Antunes, M.T., Castanhinha, R., Fröbisch, J., and Martins, R.M.S. (2018). *Endothiodon* cf. *bathystoma* (Synapsida: Dicynodontia) bony labyrinth anatomy, variation and body mass estimates. PLoS One *13*, e0189883. https://doi.org/10.1371/journal.pone.0189883.

49. Ekdale, E.G. (2013). Comparative anatomy of the bony labyrinth (inner ear) of placental mammals. PLoS One *8*, e66624. https://doi.org/10.1371/journal.pone.0066624.

50. Wever, E.G. (1978). The Reptile Ear: Its Structure and Function (Princeton University Press).

51. Manley, G.A. (1990). Peripheral Hearing Mechanisms in Reptiles and Birds (Springer Berlin).

52. Manley, G.A. (2000). The hearing organs of lizards. In Comparative Hearing: Birds and Reptiles, R.J. Dooling, R.R. Fay, and A.N. Popper, eds. (Springer New York), pp. 139–196.

53. Dooling, R.J., Lohr, B., and Dent, M.L. (2000). Hearing in birds and reptiles. In Comparative Hearing: Birds and Reptiles, R.J. Dooling, R.R. Fay, and A.N. Popper, eds. (Springer New York), pp. 308–359.

54. Wever, E.G., Herman, P.N., Simmons, J.A., and Hertzler, D.R. (1969). Hearing in the blackfooted penguin, *Spheniscus demersus*, as represented by the cochlear potentials.

Proc. Natl. Acad. Sci. USA *63*, 676–680. https://doi.org/10.1073/pnas.63.3.676.

55. Manley, G.A., Köppl, C., and Yates, G.K. (1997). Activity of primary auditory neurons in the cochlear ganglion of the emu *Dromaius novaehollandiae*: spontaneous discharge, frequency tuning, and phase locking. J. Acoust. Soc. Am. *101*, 1560–1573. https://doi.org/10.1121/1.418273.

56. Sobral, G., Reisz, R.R., Neenan, J.M., Müller, J., and Scheyer, T.M. (2016). Basal reptilians, marine diapsids, and turtles: the flowering of reptile diversity. In Evolution of the Vertebrate Ear – Evidence from the Fossil Record, J.A. Clack, R.R. Fay, and A.N. Popper, eds. (Springer New York), pp. 207–243.

57. Kemp, T.S. (2007). Acoustic transformer function of the postdentary bones and quadrate of a nonmammalian cynodont. J. Vertebr. Paleontol. *27*, 431–441. https://doi.org/10.1671/0272-4634(2007)27.

58. Ekdale, E.G. (2016). The ear of mammals: from monotremes to humans. In Evolution of the Vertebrate Ear – Evidence from the Fossil Record, J.A. Clack, R.R. Fay, and A.N. Popper, eds. (Springer New York), pp. 175–206.

59. Sobral, G., and Müller, J. (2016). Archosaurs and their kin: the ruling reptiles. In Evolution of the Vertebrate Ear – Evidence from the Fossil Record, J.A. Clack, R.R. Fay, and A.N. Popper, eds. (Springer New York), pp. 285–326.

60. Gower, D.J., and Walker, A.D. (2002). New data on the braincase of the aetosaurian archosaur (Reptilia: Diapsida) *Stagonolepis robertsoni* Agassiz. Zool. J. Linn. Soc. *136*, 7–23. https://doi.org/10.1046/j.1096-3642.2002.00023.x.

61. Bever, G.S., Bell, C.J., and Maisano, J.A. (2005). The ossified braincase and cephalic osteoderms of *Shinisaurus crocodilurus* (Squamata, Shinisauridae). Palaeontol. Electron. *8*, 4A.

62. Olroyd, S.L., and Sidor, C.A. (2022). Nomenclature, comparative anatomy, and evolution of the reflected lamina of the angular in non-mammalian synapsids. J. Vertebr. Paleontol. *42*, e2101923. https://doi.org/10.1080/02724634.2022.2101923.

63. Gower, D.J., and Weber, E. (1998). The braincase of *Euparkeria*, and the evolutionary relationships of birds and crocodiles. Biol. Rev. Camb. Philos. Soc. *73*, 367–411. https://doi.org/10.1017/S0006323198005222.

64. Evans, S.E. (2016). The lepidosaurian ear: variations on a theme. In Evolution of the Vertebrate Ear: Evidence from the Fossil Record, J.A. Clack, R.R. Fay, and A.N. Popper, eds. (Springer New York), pp. 245–284.

65. Heaton, M.J. (1979). Cranial anatomy of primitive reptiles from the late pennsylvanian and early permian Oklahoma and Texas. OGS (Obstet. Gynecol. Surv.) *127*, 1–84.

66. Gardner, N.M., Holliday, C.M., and O'Keefe, F.R. (2010). The braincase of *Youngina capensis* (Reptilia, Diapsida): new insights from high-resolution CT scanning of the holotype. Palaeontol. Electron. *13*, 19A.

67. Bazzana, K.D., Evans, D.C., Bevitt, J.J., and Reisz, R.R. (2023). Endocasts of the basal sauropsid *Captorhinus* reveal unexpected neurological diversity in early reptiles. Anat. Rec. *306*, 552–563. https://doi.org/10.1002/ar.25100.

STAR★METHODS

KEY RESOURCES TABLE

REAGENT or RESOURCE	SOURCE	IDENTIFIER
Deposited data		
Raw CT data	This paper	https://www.morphosource.org/concern/media/000441468?locale=en
Software and algorithms		
phytools v.1.0-3	R v.4.1.3	
ape v.5.6-2	R v.4.1.3	
castor v.1.7.6	R v.4.1.3	

RESOURCE AVAILABILITY

Lead contact

Further information and requests should be directed to the lead contact, Kayla Bazzana-Adams (kayla.bazzana@mail.utoronto.ca).

Materials availability

Unprocessed 16-bit TIFF slices are available online through MorphoSource (https://www.morphosource.org/concern/media/000441468?locale=en).

Data and code availability

- Data used in the ancestral state reconstruction analyses are available in Data S1 the supplemental information for this paper, or from the lead contact.
- R code used to perform the ancestral state reconstruction analyses is available on Zenodo: https://doi.org/10.5281/zenodo.7745782, or from the lead contact.
- Any additional information required to reanalyze the data reported in this paper is available from the lead contact upon request.

EXPERIMENTAL MODEL AND SUBJECT DETAILS

CT scanning

We scanned an isolated braincase of *Dimetrodon* cf. *loomisi* (FMNH UC 423) from the Craddock Bonebeds of Texas. Details regarding the scanning procedure used in this study are provided in the "scanning" subsection of the methods section.

METHOD DETAILS

Details regarding the segmentation method used in this study are detailed in the "scanning" sub-section of the methods section. The height and width of each canal were measured with the inner ear oriented such that the plane of the canal being measured was flat relative to the viewer, with height measured as the distance from the distalmost point of the canal arc from the vestibule, to the vestibule wall directly below that point (see Figure 2 in Benoit et al.[7] for illustration of these measurements). The radius of curvature for each canal was then calculated as $r = 0.5*((H+W)/2)$. Eccentricity was calculated as $e = \sqrt{(1-(\text{minor axis}/\text{major axis})^2)}$ (see Goyens[26] for visual illustration of the major vs minor axes). Canal length was calculated by summing the distances of a spline taken along the centre of each canal; detailed protocol for length calculations, along with visual aids, are available from the lead contact. Brain flexure was measured with endocasts in lateral view.

QUANTIFICATION AND STATISTICAL ANALYSIS

Ancestral state reconstructions were performed in *R Studio* using the function *ace* for the maximum likelihood analyses, and the function *hsp_parsimony* for the parsimony analyses.